

Fluorescence Switching via Competitive ESIPT and Spirolactam Ring Opening in a Multifunctional Rhodamine B Probe for Selective Detection of Cu²⁺ and OCl⁻: Theoretical Insights with Anticancer and Biosensor Activity

Vishnu S^a Avijit Kumar Das^{a*} Gouri Karan^b, Sujata Maiti Choudhury^b

^aDepartment of Chemistry, Christ University, Hosur Road, Bangalore, Karnataka, 560029 India

*Email: avijitkumar.das@christuniversity.in

^bCancer Nanotherapeutics Laboratory, Biochemistry, Molecular Endocrinology, and Reproductive Physiology Division, Department of Human Physiology, Vidyasagar University, Midnapore- 721 102, West Bengal, India

1. Experimental

1.1. General:

Unless otherwise mentioned, chemicals and solvents were purchased from Sigma-Aldrich chemicals Private Limited and were used without further purification. $^1\text{H-NMR}$ spectra were recorded on Bruker 400 MHz instrument. For NMR spectra, $\text{d}^6\text{-DMSO}$ was used as solvent using TMS as an internal standard. Chemical shifts are expressed in δ - units and $^1\text{H-}^1\text{H}$ and $^1\text{H-C}$ coupling constants in Hz. UV-vis titration experiments were performed on a UV-Spectrophotometer: PerkinElmer, Lambda 30 and fluorescence experiment was done using Shimadzu RF-5301PC Fluorescence spectrofluorometer using a fluorescence cell of 10 mm path.

1.2. General method of UV-vis and fluorescence titration:

By UV-vis method:

For UV-vis titrations, stock solution of the sensor was prepared ($c = 2 \times 10^{-5} \text{ M}$) in $\text{CH}_3\text{CN-HEPES}$ buffer (9/1, v/v, 25°C) at pH 7.4. The solution of the guest interfering analytes like Ni^{2+} , Mn^{2+} , Pb^{2+} , Cd^{2+} , Fe^{2+} , Cu^{2+} , Fe^{3+} , Zn^{2+} , Co^{2+} , Al^{3+} , Hg^{2+} as their chloride salts were also prepared in the order of $c = 2 \times 10^{-4} \text{ M}$. Solutions of various concentrations containing sensor and increasing concentrations of cations were prepared separately. The spectra of these solutions were recorded by means of UV-vis methods. For UV-vis titrations with ct-DNA and BSA, stock solution of the sensor was prepared ($c = 2 \times 10^{-5} \text{ M}$) in DMSO- Tris-HCl buffer (40 μL in 2 ml Tris-HCl buffer) at pH 7.2. Tris-HCl buffer was used to prepare the solution of ct-DNA (2 mM in base pairs) and BSA ($c = 7.4 \mu\text{M}$). The spectra of these solutions were recorded by means of UV-vis methods.

General procedure for drawing Job plot by UV-vis method:

Stock solution of same concentration of **BHS** and Cu^{2+} were prepared in the order of $\approx 2.0 \times 10^{-5} \text{ M}$ in $\text{CH}_3\text{CN-HEPES}$ buffer (9:1, v/v, pH = 7.4). The absorbance in each case with different *host-guest* ratio but equal in volume was recorded. Job plots were drawn by plotting $\Delta I \cdot X_{\text{host}}$ vs X_{host} (ΔI = change of intensity of the absorbance spectrum during titration and X_{host} is the mole fraction of the host in each case, respectively).

By fluorescence method:

For fluorescence titrations, stock solution of the sensor ($c = 2 \times 10^{-5} \text{ M}$) was prepared for the titration of cations in $\text{CH}_3\text{CN-HEPES}$ buffer [9:1, v/v, pH = 7.4]. The solution of the guest cations using their chloride salts in the order of 200 μM were also prepared. Solutions of various concentrations containing sensor and increasing concentrations of cations were prepared separately. The spectra of these solutions were recorded by means of fluorescence

methods. For UV-vis titrations with ct-DNA and BSA, stock solution of the sensor was prepared ($c = 2 \times 10^{-5}$ M) in DMSO- Tris-HCl buffer (40 μ L in 2 ml Tris-HCl buffer) at pH 7.2. Tris-HCl buffer was used to prepare the solution of ct-DNA (2 mM in base pairs) and BSA ($c = 7.4 \mu$ M). The spectra of these solutions were recorded by means of UV-vis methods.

1.3 Materials and methods for biological study:

Reagents:

Dulbecco's modified Eagle's medium (DMEM), and foetal bovine serum (FBS) were purchased from Gibco, Invitrogen, Carlsbad, CA. Antibiotic-antimycotic solution, 3-(4,5 dimethyl-2-thiazolyl)- 2,5-diphenyl-tetrazolium bromide (MTT), 5-fluorouracil (5-FU) were acquired from Sigma Aldrich Co. St. Louis, US.

In vitro cytotoxicity study on HCT-116 cells by MTT assay:

HCT-116 colorectal cancer cell line was collected from Chittaranjan National Cancer Institute, Kolkata, and was cultured in FBS (10%) and antibiotic-antimycotic solution supplemented DMEM medium in a humidified CO₂ incubator. To study dose-dependent cytotoxicity, 100 μ l DMEM containing 1×10^5 cells was seeded in each well of a 96-well plate. After 24 hours of incubation, different concentrations (5, 10, 50, 100, 250 μ M) of **BHS** solution were added to the respective wells and further incubated for 24 hours. Then, 10 μ l of 3-(4, 5-dimethylthiazol-2-yl)-2S-diphenyltetrazolium salt (5mg/ml) was added and incubated at 37°C to precipitate formazan crystals. The precipitate was solubilized by DMSO (100 μ l), and the optical density was measured at 570 nm by a Microplate reader (Bio-Rad, Model 680).¹ Standard anticancer drug 5-fluorouracil was used as a positive control. Cell viability was calculated from the following formula:

$$\text{Percentage of viable cells} = \frac{(\text{Optical density of BHS treated sample} \times 100)}{\text{Optical density of negetive control}}$$

Fluorescence imaging study:

To study the copper (Cu²⁺) and hypochlorite (OCl⁻) analyte sensing activity of **BHS** in biological samples, a fluorescence imaging study was conducted on HCT-116 colorectal carcinoma cells. Sub-cultured HCT-116 cells (cell count 1×10^6 cells/ml) were treated with 50 μ M **BHS** solution for 6 hours, followed by incubation with 25 μ M copper (Cu²⁺) and hypochlorite (OCl⁻) solution for 1 hour. Then, cells were washed with phosphate-buffered

saline, and fluorescence images of untreated, **BHS**, **BHS/ Cu²⁺**, and **BHS/OCl⁻**-treated cells were captured by a fluorescence microscope (Leica DFC 295, Germany).²

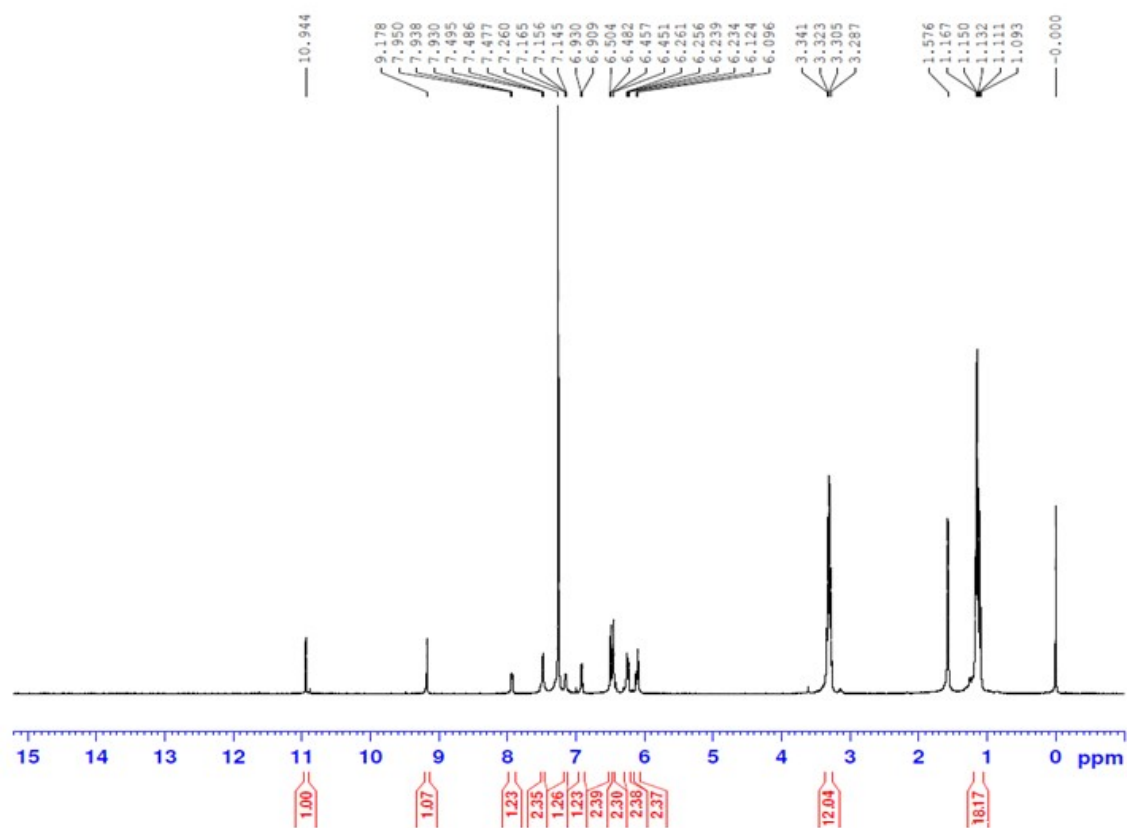


Figure S1. ¹H NMR spectrum of **BHS**

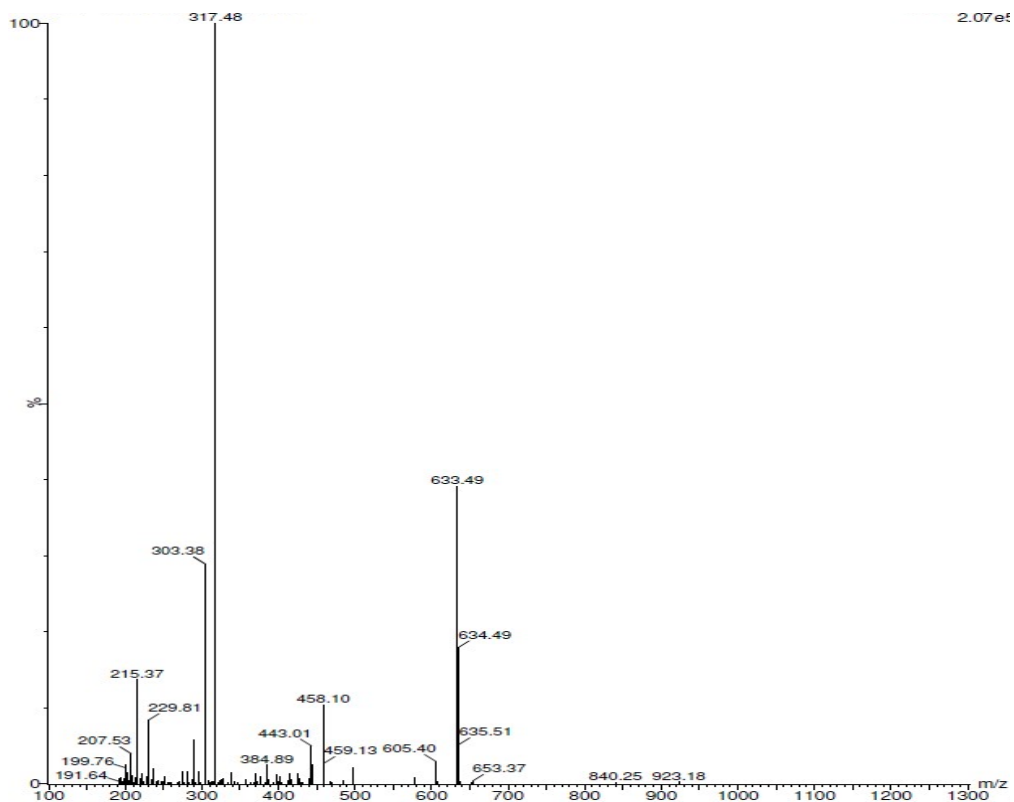


Figure S2. Mass spectrum of BHS

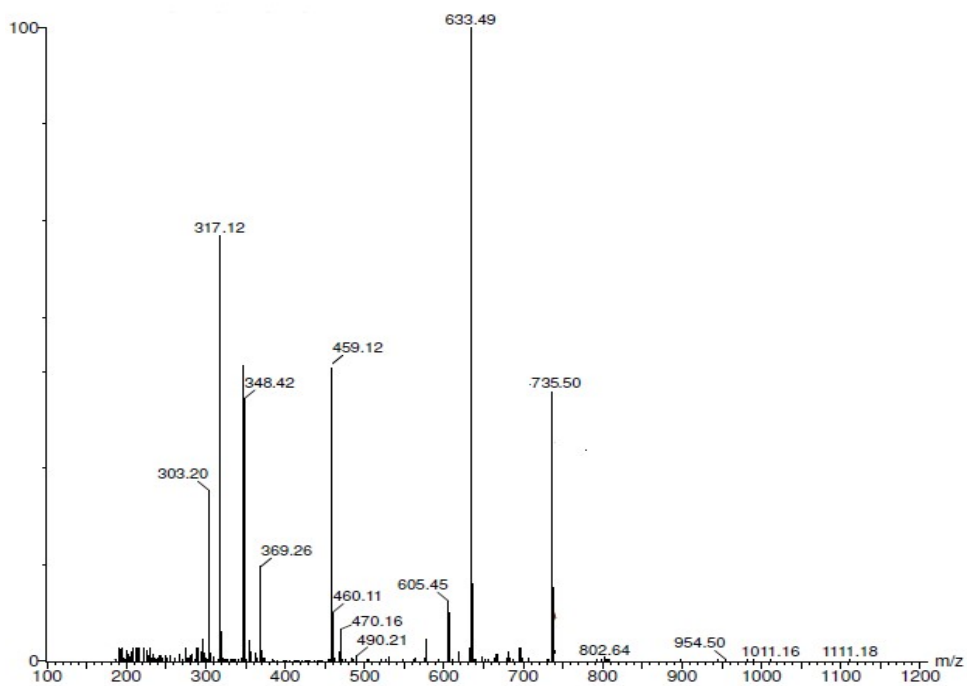


Figure S3. Mass spectrum of BHS+Cu²⁺ complex

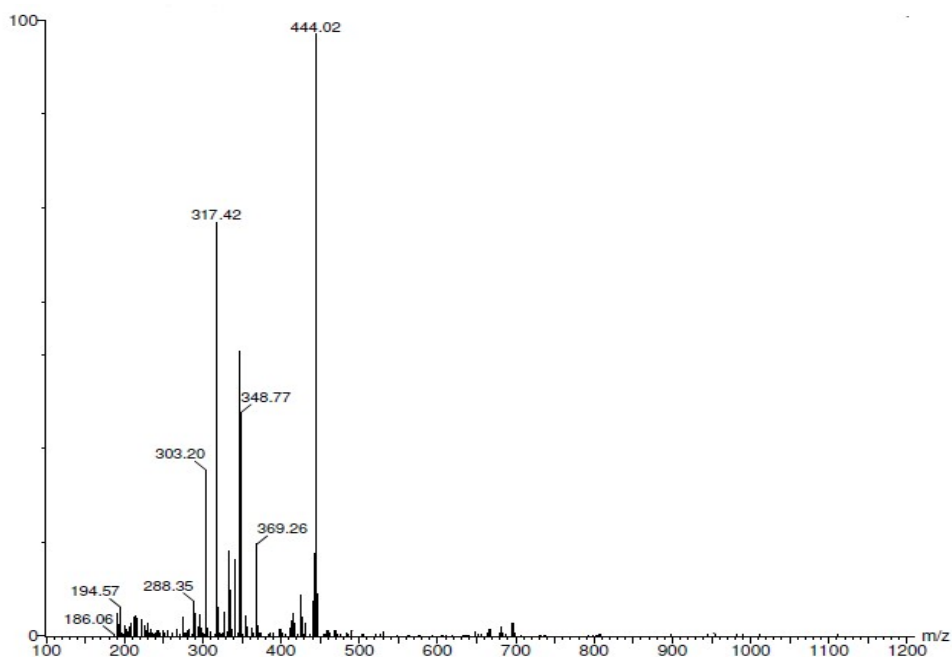


Figure S4. Mass spectrum of **BHS+OCl⁻** complex

2. Calculation of the detection limit (DL):

The detection limit DL of **BHS** for **Cu²⁺** was determined from the following equation:

$$DL = K * Sb1/S$$

Where $K = 2$ or 3 (we take 3 in this case); $Sb1$ is the standard deviation of the blank solution; S is the slope of the calibration curve.

From the graph Fig.S4, we get slope = 12716 , and $Sb1$ value is 26738.15 .

Thus, using the formula we get the Detection Limit for **Cu²⁺** = $6.30 \mu\text{M}$.

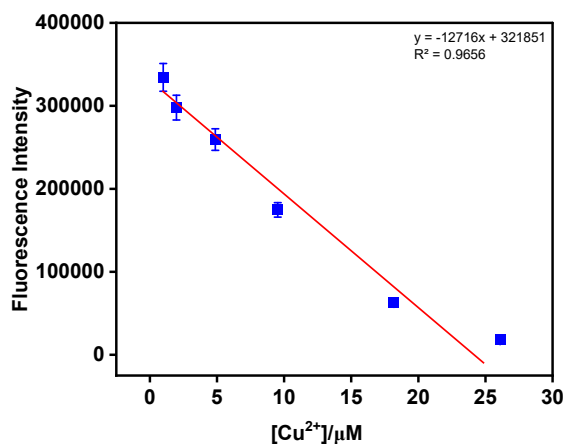


Figure S5. Changes of fluorescence intensity of **BHS** as a function of **[Cu²⁺]** at 576 nm .

The detection limit DL of **BHS** for OCI^- was determined from the following equation:

$$\text{DL} = K * \text{Sb1}/S$$

Where $K = 2$ or 3 (we take 3 in this case); Sb1 is the standard deviation of the blank solution; S is the slope of the calibration curve.

From the graph Fig.S6, we get slope = 6261.2 , and Sb1 value is 17151.46 .

Thus, using the formula we get the Detection Limit for $\text{OCI}^- = 8.21 \mu\text{M}$.

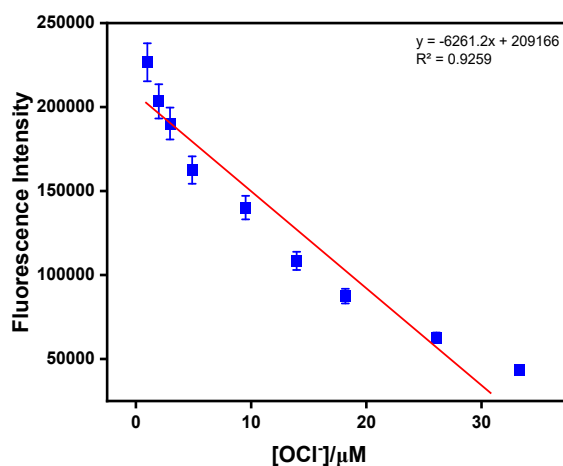


Figure S6. Changes of Fluorescence Intensity of **BHS** as a function of $[\text{OCI}^-]$ at 576 nm .

The detection limit (DL) of **BHS** - Cu^{2+} complex with DNA and BSA was determined from the following equation:

$$\text{DL} = K * \text{Sb1}/S$$

Where $K = 2$ or 3 (we take 3 in this case); Sb1 is the standard deviation of the blank solution; S is the slope of the calibration curve.

From fluorescence titration of **BHS** - Cu^{2+} complex with DNA (Fig.S7), slope values are -0.0103 and Sb1 value is 47.1712 .

From and fluorescence titration of **BHS** - Cu^{2+} complex with BSA (Fig.S7), slope values are -0.4464 and Sb1 values are 56.64 .

Thus, using the formula we have calculated the detection limit for **BHS** - Cu^{2+} complex with DNA from fluorescence titration $13.15 \mu\text{M}$. And **BHS** - Cu^{2+} complex with BSA from fluorescence titration $23.08 \mu\text{M}$ respectively.

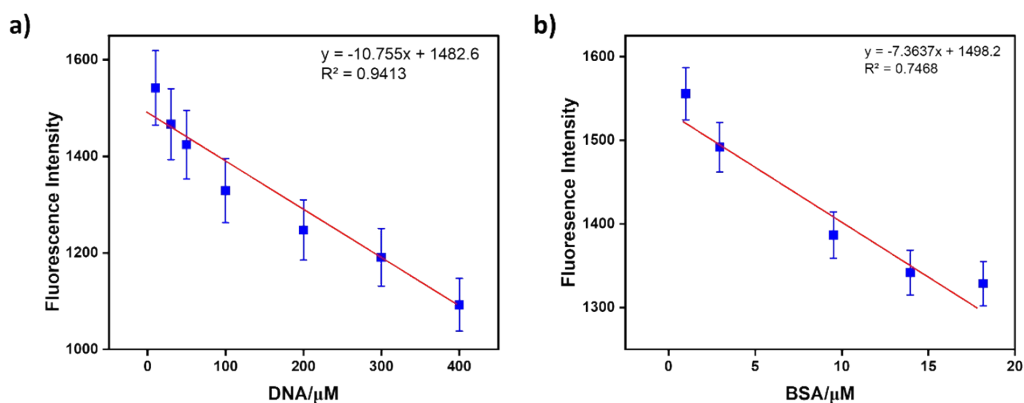


Figure S7. Changes of emission at 576 nm (a) of **BHS** -Cu²⁺ complex ($c = 2.0 \times 10^{-5}$ M) upon addition of ct DNA ($c = 2$ mM in base pairs). Changes of emission at 576 nm (b) of **BHS** -Cu²⁺ complex ($c = 2.0 \times 10^{-5}$ M) upon addition of BSA ($c = 7.4$ μM).

3. Jobs plot analysis:

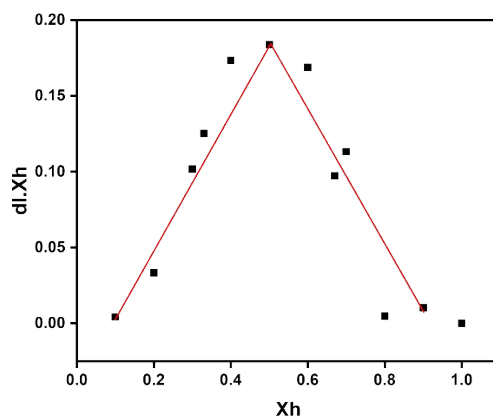


Figure S8. Job's plot diagram of receptor **BHS** for Cu²⁺ (where X_h is the mole fraction of host **BHS** and ΔI indicates the change of the intensity).

4. Binding constant determination:

The binding constant value of cation Cu²⁺ with the sensor has been determined from the emission intensity data following the modified Benesi–Hildebrand equation, $1/\Delta I = 1/\Delta I_{\max} + (1/K[C])(1/\Delta I_{\max})$. Here $\Delta I = I - I_{\min}$ and $\Delta I_{\max} = I_{\max} - I_{\min}$, where I_{\min} , I , and I_{\max} are the emission intensities of sensor considered in the absence of guest, at an intermediate concentration and at a concentration of complete saturation of guest where K is the binding constant and $[C]$ is the guest concentration respectively. From the plot of $(I_{\max} - I_{\min})/(I - I_{\min})$ against $[C]^{-1}$ for sensor, the value of K has been determined from the slope. The association constant (K_a) as determined by fluorescence titration method for sensor with Cu²⁺ is found to be $2.73 \times 10^5 \text{ M}^{-1}$ (error < 10%).

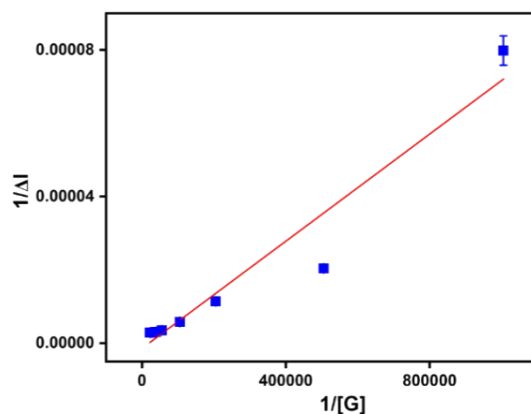


Figure S9. Benesi–Hildebrand plot from fluorescence titration data of receptor **BHS** (20 μ M) with Cu^{2+} [G].

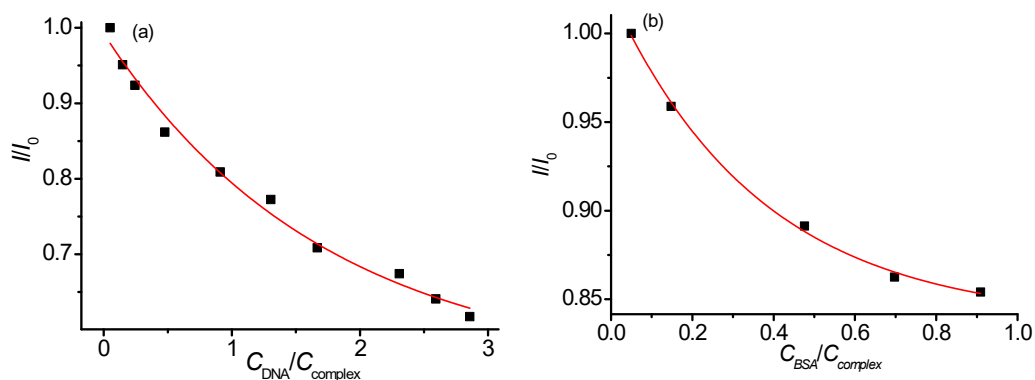


Figure S10. Non-linear fitting curves of binding isotherms resulting from spectrofluorometric titrations of **BHS**+ Cu^{2+} complex for the determination of binding constants (K_b) with ct DNA (a) and BSA(b). Red lines represent the best fits to the theoretical model.

The binding constants of **BHS**+ Cu^{2+} complex with ct DNA and BSA were determined from the fluorometric titration spectra by non-linear fitting of the experimental data to the theoretical model in the following equation:³

$$\frac{I}{I_0} = 1 + \frac{Q-1}{2} \left(A + xn + 1 - \sqrt{(Q + xn + 1)^2 - 4xn} \right) \quad (\text{Equation 1})$$

where $Q = I/I_0$ is the minimal emission intensity in the presence of excess ligand; n is the number of independent binding sites.

$$A = 1/(K_b \times C_{\text{Lig or complex}});$$

$$x = C_{\text{Cu}^{2+} \text{ or DNA or BSA}}/C_{\text{Lig or complex}} \text{ is the titration variable}$$

5. Computational details:

Density Functional Theory (DFT)⁴ calculations were conducted using the Gaussian 09 (Revision A.02) package, with "Gauss View" utilized for visualizing molecular orbitals. Becke's three-parameter hybrid-exchange functional, the Lee-Yang-Parr expression for nonlocal correlation, and the Vosko-Wilk-Nuair 1980 local correlation functional (B3LYP) were employed in the calculation.⁵ Optimization of **BHS** and single-point energy calculations in the gas phase were performed using the 6-31+(g) basis set. The Lanl2dz basis set was used for Cu^{2+} and for H atoms we used 6-31+(g) basis set; for C, N, O, Cu atoms we employed LanL2DZ as basis set for all the calculations. The calculated electron-density plots for frontier molecular orbitals were prepared by using Gauss View 5.1 software. All the calculations were performed with the Gaussian 09W software package.⁶

6. pH Study:

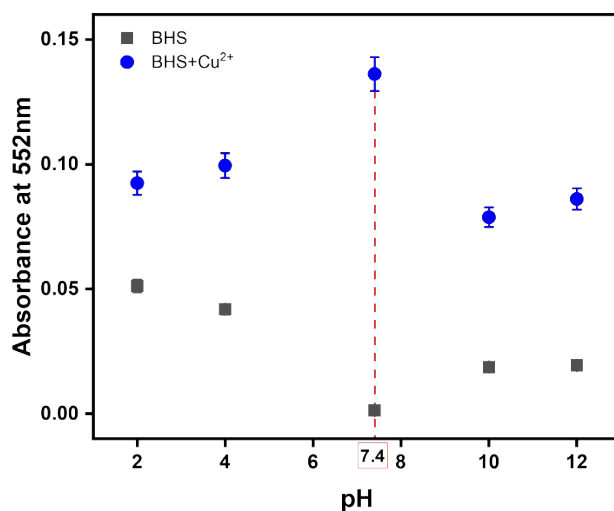
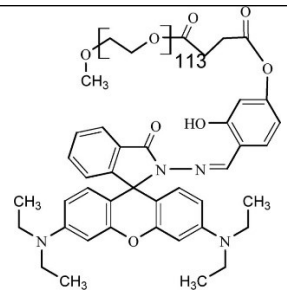
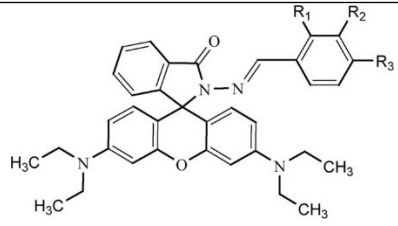
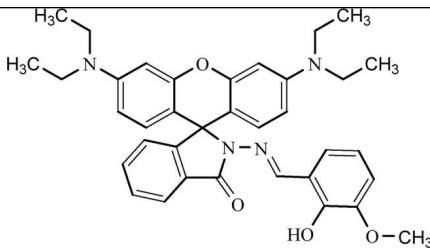
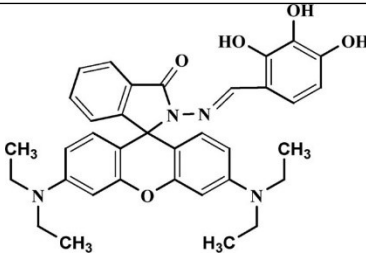
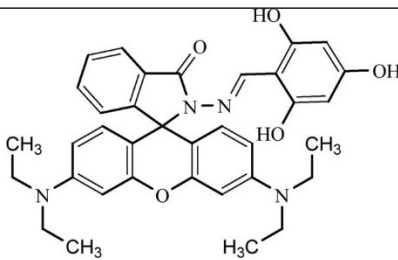
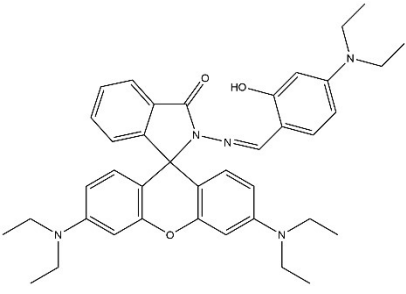


Figure S11. Changes in absorbance of **BHS** and **BHS+Cu²⁺** ($c = 2 \times 10^{-5}\text{M}$) at different pH.

7. Comparison table with the reported rhodamine based chemosensors:

Serial no.	Probe	Analyte	Probe type	Detection limit	Applications	Ref.
1		Cu ²⁺	Colorimetric and fluorescent sensor	2.5 × 10 ⁻⁸ M	Real Sample analysis	7
2		Cu ²⁺	Colorimetric and fluorescent sensor	0.25 μM [RB1], 0.15 μM [RB2] and 0.18 μM [RB3]	Bioimaging and Real Sample analysis	8
3		Cu ²⁺	Colorimetric sensor	4.0 × 10 ⁻² μM	Test strips, cytotoxicity and live cell imaging	9
4		Cu ²⁺	Colorimetric sensor	0.1398 μM	Test strips and cytotoxicity	10
5		Cu ²⁺	Colorimetric sensor	0.48 μM	Test strips and cytotoxicity	11

6		Cu ²⁺ and OCl ⁻	Fluorescent and colorimetric sensor	2.61 μM and 1.96 μM	ESIPT probe, Dual sensor, Dipstick Method, DNA and Protein Binding Study. In-Silico Molecular Docking Study	Current Work
---	---	---------------------------------------	-------------------------------------	---------------------	---	--------------

10. References:

1. A. D. Chaudhuri, S. Mondal, R. Mahata, S. Manna, A. Majumder, S. K. Dey, D. Giri, T. Roy, R. N. Baral, S. Roy, B. Saha, *International Journal of Biological Macromolecules*. 2025, 306, 141741.
2. B. Das, K. C. Murmu, S. K. Dey, S. M. Chaudhuri, Z. M. Almarhoon, M. Z. Ansari, P. P. Bag, M. Dolai, *Inorganic Chemistry Communications*. 2024, **170**, 113108.
3. F. H. Stootman, D. M. Fisher, A. Rodger, J. R. Aldrich-Wright, *Analyst.*, 2006, 131, 1145.
4. R. G. Parr and W. Yang, *Density Functional Theory of Atoms and Molecules*, Oxford University Press, 1989, Oxford.
5. (a) A. D. Becke, *J. Chem. Phys.*, 1993, 98 5648. (b) C. Lee, W. Yang and R. G. Parr, *Phys. Rev. B*, 1998, 37, 785.
6. M. J. Frisch, G. W. Trucks, H. B. Schlegel, G. E. Scuseria, M. A. Robb, J. R. Cheeseman, G. Scalmani, V. Barone, B. Mennucci, G. A. Petersson, H. Nakatsuji, M. Caricato, X. Li, H. P. Hratchian, A. F. Izmaylov, J. Bloino, G. Zheng, J. L. Sonnenberg, M. Hada, M. Ehara, K. Toyota, R. Fukuda, J. Hasegawa, M. Ishida, T. Nakajima, Y. Honda, O. Kitao, H. Nakai, T. Vreven, J. A. Montgomery Jr., J. E. Peralta, F. Ogliaro, M. Bearpark, J. J. Heyd, E. Brothers, K. N. Kudin, V. N. Staroverov, R. Kobayashi, J. Normand, K. Raghavachari, A. Rendell, J. C. Burant, S. S. Iyengar, J. Tomasi, M. Cossi, N. Rega, J. M. Millam, M. Klene, J. E. Knox, J. B. Cross, V. Bakken, C. Adamo, J. Jaramillo, R. Gomperts, R. E. Stratmann, O. Yazyev, A. J. Austin, R. Cammi, C. Pomelli, J. W. Ochterski, R. L. Martin, K. Morokuma, V. G. Zakrzewski, G. A. Voth, P. Salvador, J. J. Dannenberg, S. Dapprich, A. D. Daniels, Ö. Farkas, J. B. Foresman, J. V. Ortiz, J. Cioslowski and D. J. Fox, Gaussian Inc., 2009, Wallingford CT.
7. G. Li, F. Tao, Q. Liu, L. Wang, Z. Wei, F. Zhu, W. Chen, H. Sun, Y. Zhou. *New J. Chem.*, 2016, **40**, 4513.
8. F. Yan, X. Sun, R. Zhang, Y. Jiang, J. Xu, J. Wei. *Spectrochim. Acta A Mol. Biomol. Spectrosc.*, 2019, **222**, 117222.
9. N.A.S. Pungut, M.P. Heng, H.M. Saad, K.S. Sim, V.S. Lee, K.W. Tan. *J. Mol. Struct.*, 2021, **1238**, 130453 .

10. W.C. Chan, H.M. Saad, K.S. Sim, V.S. Lee, C.W. Ang, K.Y. Yeong, K.W. Tan. *Spectrochim. Acta A Mol. Biomol. Spectrosc.*, 2021, **262**, 120099 .
11. P.W. Cheah, M.P. Heng, H.M. Saad, K.S. Sim, K.W. Tan. *Opt. Mater.*, 2021, **114**, 110990 .